Science of the Total Environment 769 (2021) 144892

Contents lists available at ScienceDirect

Science of the Total Environment

journal homepage: www.elsevier.com/locate/scitotenv

Significant mercury efflux from a Karst region in Southwest China - Results from mass balance studies in two catchments

Jicheng Xia [a], Jianxu Wang [a,b], Leiming Zhang [c], Xun Wang [d], Wei Yuan [a], Christopher W.N. Anderson [e], Chaoyue Chen [a,f], Tao Peng [a,g], Xinbin Feng [a,b,*]

[a] State Key Laboratory of Environmental Geochemistry, Institute of Geochemistry, Chinese Academy of Sciences, Guiyang 550081, China
[b] CAS Centre for Excellence in Quaternary Science and Global Change, Xi'an 710061, China
[c] Air Quality Research Division, Science and Technology Branch, Environment and Climate Change Canada, Toronto M3H5T4, Canada
[d] College of Resources and Environment, Southwest University, Chongqing 400715, China
[e] Environmental Sciences Group, School of Agriculture and Environment, Massey University, Private Bag 11 222, Palmerston North 4442, New Zealand
[f] University of Chinese Academy of Sciences, Beijing 100049, China
[g] Puding Karst Ecosystem Research Station, Chinese Academy of Sciences, Puding 562100, China

HIGHLIGHTS

- The two studied karst catchments were distinct Hg sources.
- The Hg geologic setting governs intensity of Hg geochemistry process in karst region.
- Air-surface exchange and crops cultivation played important roles in shaping Hg fate.

GRAPHICAL ABSTRACT

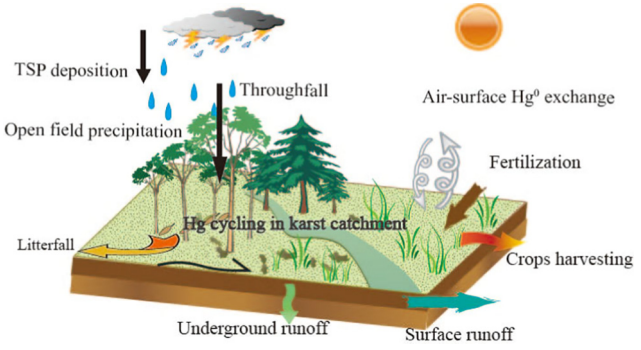

ARTICLE INFO

Article history:
Received 13 November 2020
Received in revised form 23 December 2020
Accepted 28 December 2020
Available online 14 January 2021

Editor: Jay Gan

Keywords:
Atmospheric Hg cycling
Air-surface exchange
Mass balance
Karst catchment

ABSTRACT

Karst regions have long been recognised as landscapes of ecological vulnerability, however the mass balance and fate of mercury (Hg) in karst regions have not been well documented. This study focused on the largest contiguous karst area in China and investigated Hg mass balance in two catchments, one with high geological Hg (Huilong) and the other representative of regional background Hg (Chenqi). The mass balance of Hg was calculated separately for the two catchments by considering Hg in throughfall, open field precipitation, total suspended particulate matter (TSP), litterfall, fertilizer, crop harvesting, air-surface Hg^0 exchange, surface runoff and underground runoff. Results show that litterfall Hg deposition is the largest loading (from atmosphere) of Hg in both catchments, accounting for 61.5% and 38.5% of the total Hg input at Huilong and Chenqi, respectively. Air-surface Hg^0 exchange is the largest efflux, accounting for 71.7% and 44.6% of the total Hg output from Huilong and Chenqi, respectively. Because both catchments are subject to farm and forest land use, cultivation plays an important role in shaping Hg fate. Mercury loading through fertilizer was ranked as the second largest input (28.5%) in Chenqi catchment and Hg efflux through crop harvest was ranked as the second largest output pathway in both Huilong (27.0%) and Chenqi (52.9%). The net Hg fluxes from the catchments are estimated to be 1498 ± 1504 μg m^{-2} yr^{-1} and 4.8 ± 98.2 μg m^{-2} yr^{-1}. The significantly greater magnitude of net Hg source in Huilong is attributed to higher air-surface Hg^0 exchange. The output/input ratio of Hg in this study was much greater than has been reported for other forest or agricultural ecosystems and indicates that the karst region of Southwest

* Corresponding author at: State Key Laboratory of Environmental Geochemistry, Institute of Geochemistry, Chinese Academy of Sciences, Guiyang 550081, China.
E-mail address: fengxinbin@vip.skleg.cn (X. Feng).

https://doi.org/10.1016/j.scitotenv.2020.144892

China is a significant source of atmospheric Hg. The results of this study should be considered in the development of pollution control policies which seek to conserve fragile karst ecosystems characterised by high geological background of Hg.

1. Introduction

Mercury (Hg) is a toxic, bioaccumulative, and volatile heavy metal, and can transform into more toxic species, i.e., methylmercury (MeHg) in the environment (Barkay and Wagner-Dobler, 2005; Hong et al., 2013). Mercury biogeochemical processes in terrestrial and aquatic ecosystems have therefore been investigated extensively worldwide. Existing Hg catchment-scale mass balance models are mainly based on measured and estimated Hg fluxes at various input/output locations, and such models are useful tools for deriving source-sink relationships, and for assessing associated historical or future environmental impacts in different ecosystems (Gao et al., 2006; Lessard et al., 2013; Macleod et al., 2005). Most research on Hg mass balance in terrestrial ecosystems has focused on the biogeochemical cycle of Hg in forest ecosystems at regional to global scales (Ma et al., 2016; Nelson et al., 2007). For example, in a subtropical forest in southwest China, Hg input by throughfall and litterfall were estimated to be 32.2 and 42.9 μg m^{-2} yr^{-1}, respectively, while Hg output was found to be dominated by fluxes across the soil-air interface (18.6 μg m^{-2} yr^{-1}) and runoff and/or stream flow (7.2 μg m^{-2} yr^{-1}) (Ma et al., 2016).

To date, studies on Hg biogeochemical processes in environmentally fragile regions such as karst landscapes have been limited (Ci et al., 2014; Liu et al., 2019). Karst landscapes worldwide have long been recognised for their ecological vulnerability (Jiang et al., 2014). Soil erosion is generally severe in karst areas, and this may lead to the loss of a large amount of soil Hg. In addition, due to the limited availability of arable land in karst areas, forest lands are at risk of conversion to farmland, and this may aggravate soil erosion while at the same time increasing Hg input through fertilization. Therefore, the biogeochemical cycle of Hg in karst ecosystems may be different from those in the other terrestrial ecosystems.

China has the largest karst areas (1.3 million km^2) in the world, accounting for 13.5% of the global total. Nearly half of China's karst landscape (0.62 million km^2) is distributed in Southwest China (Huang et al., 2008). Mercury concentrations in the top (0–25 cm) and deep soils (below 100 cm or C-horizon) of the karst area in southwest China are reported to be 3 to 5 times higher than those in the other geographical landscapes in China (Nie et al., 2019). Such elevated soil Hg concentrations in Southwest China are known to be a function of the high geochemical Hg background due to the extensive and continued mining activities that occurred during 1640–1970 (Liu et al., 2019; Wang et al., 2005). The karst area in Southwest China is located in the global Hg mineralization belt and is also part of China's "large area of low temperature mineralization in Southwest China." This is the region with the most abundant Hg mineral resources in China, with several well-known Hg mines such as the Wanshan Hg Mine, Wuchuanmu Hg Mine, Danzhai Hg Mine and Lanmuchang Hg Mine. The mining and smelting of Hg and other mineral resources has released large amounts of Hg to the air and the Earth's surface environment. Areas with severe Hg pollution caused by Hg mining and local smelting have shown strong atmospheric Hg deposition, e.g., up to 6178 μg m^{-2} yr^{-1} (Dai et al., 2012).

Given the elevated Hg concentrations in karst surface soils of Southwest China, we suspect that the karst region of Southwest China remains a distinct Hg source, despite the enhanced environmental protection policies in recent years that have sealed pollution from areas of historic mine waste Hg mining areas (Li et al., 2012; Yan et al., 2019). To verify this hypothesis, we assessed the Hg mass balance and input/output pathways including throughfall (rainfall under the forest), open field precipitation (rainfall in the open field), litterfall, TSP (total suspended particles), fertilizer, crops harvesting, air-surface Hg^0 exchange, surface runoff and underground runoff, in two selected catchments in this region. Implications of the results from this study on the management of Hg pollution in karst regions are also discussed.

2. Materials and methods

2.1. Sampling areas

We chose two karst catchments, which are geologically representative of the karst landscapes in Southwest China, to assess the mass balance of Hg (Fig. 1). The two catchments, Huilong and Chenqi, were evolved from detrital sandstone and limestone, respectively (Sun et al., 2012; Zhao et al., 2010). The Huilong catchment (25°32′N, 105°31′E) in southwest Guizhou has a size of 18 ha and an elevation of 1400–1600 m, and is located at the margin of Lanmuchang Hg—Tl mine. Mean annual air temperature is 15.2 °C and precipitation is 1315 mm. Soil Hg concentrations at the Lanmuchang Hg—Tl mine ranged from 0.41 to 610 mg kg^{-1} ($n = 31$), suggesting that Huilong catchment is contaminated with Hg (Qiu et al., 2006). For this work, Huilong catchment therefore represents a high Hg geological karst region. Chenqi catchment (26°15′N, 105°46′E) in central Guizhou has a size of 150 ha and has an elevation of 1300–1500 m. Mean annual air temperature is 15.1 °C and mean annual precipitation is almost 1378 mm. No historic or current-day Hg mining has been practiced within 50 km of this catchment, and Hg concentrations in soil, water and air in this area are used in this work to represent regional background values. The land use across the two catchments were calculated using Arc GIS 10.4. About 17% and 20% of the catchment area were used for agricultural production in Huilong and Chenqi, respectively, and forestry accounts for most of the remaining land use. Special considerations were given to the characteristics of the topography and geomorphology of both catchments when selecting the sampling sites so that the two catchments used were relatively closed with a clear boundary.

2.2. Sample collection and chemical analysis

2.2.1. Throughfall, open field precipitation and runoff sampling

Two sites in Chenqi and three sites in Huilong catchments were established to collect monthly throughfall (the part of rainfall which falls to the forest floor from the canopy) from August 2018 to July 2019. One site at each catchment was established to collect open field precipitation for the same period of throughfall. A 1.2 m^2 rain board covered with poly tetra fluoro ethylene (PTFE) was placed 0.6 m above the ground to collect rain samples (Fig. S1). A 5 L brown borosilicate glass bottle was used to collect the water sample. To avoid possible interference of litterfall and insect debris, a plastic bag was used to cover the rain board during the non-sampling period, and this bag was opened at the start of precipitation and closed at the end of precipitation. A portion of the collected precipitation sample (100 mL) was manually transferred into new polypropylene BD Falcon® centrifuge tubes, and spiked with 5 mL of ultra-clean grade HCl (BV-III grade, Beihua Chemical, China). Another 100 mL of the collected precipitation was filtered through a cellulose membrane (0.45-μm pore size, 47-mm diameter, Durapore®, Millipore) into polypropylene BD Falcon® centrifuge tubes, and then spiked with HCl (final concentration 0.5% (v: v)) for dissolved Hg (DHg) analysis. During the field procedure, ultra-pure deionized water was flushed through the precipitation collector and was then collected as a field blank solution. Three blank samples were

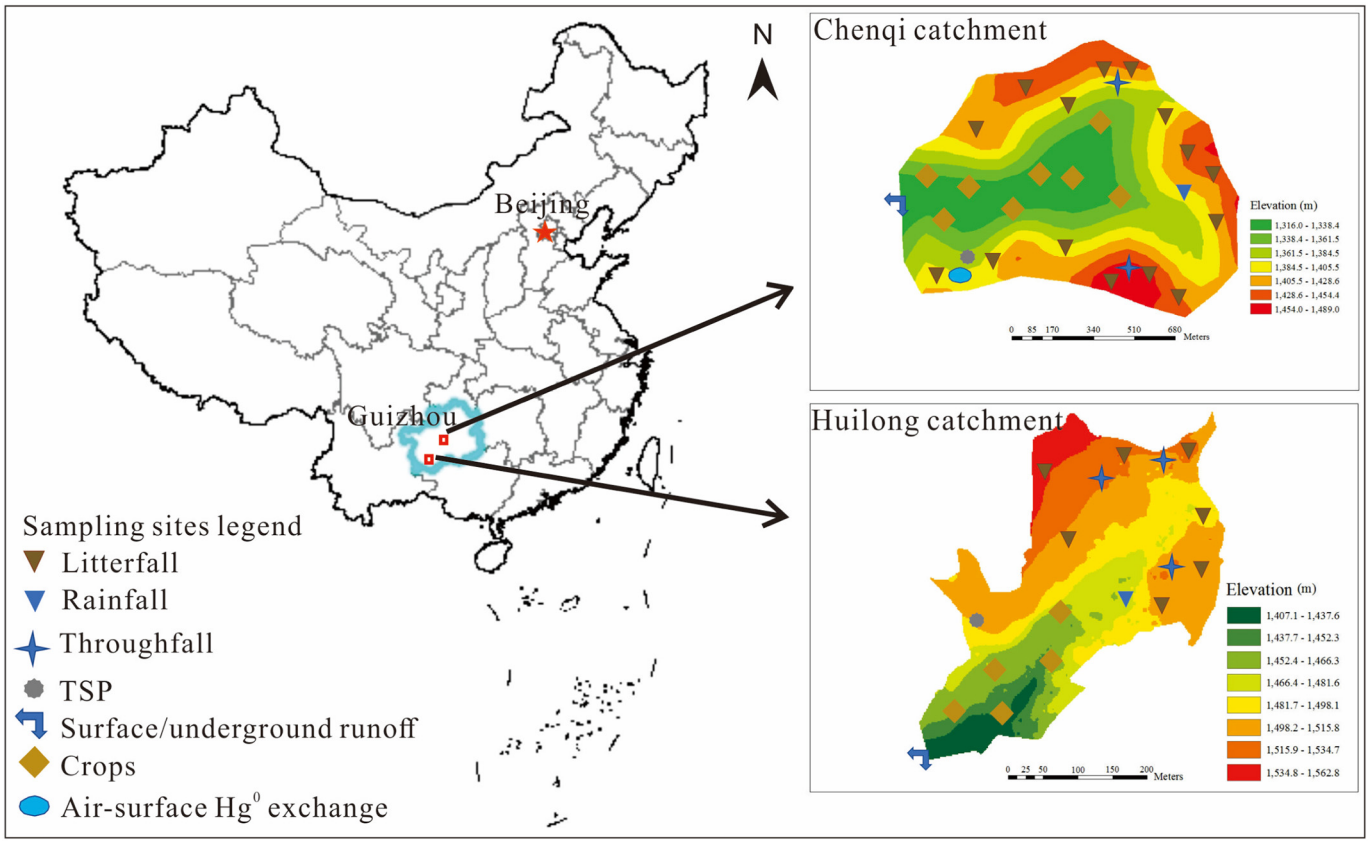

Fig. 1. Locations of Huilong (H) and Chenqi (C) catchments (marked in red square in the left panel) in Guizhou province of Southwest China.

taken every month. All precipitation samples were stored in a dark refrigerating chamber (4 °C) and transported back to a metal-free laboratory room for further processing.

Flow monitoring and sampling of surface runoff in each catchment was conducted above the surface converges of runoff. Flow monitoring and sampling of underground runoff was conducted in water heads of underground runoff at low terrain (see Figs. S2 & S3). Monthly surface runoff and underground runoff samples were collected in each catchment from August 2018 to July 2019. About 100 mL surface/underground runoff water was collected using a PTFE bottle for each outlet, and 5‰ ultra-pure hydrochloric acid was then added for acidification. Dissolved Hg (DHg) in runoff samples was analysed using the method for precipitation sampling. Surface runoff and underground runoff water samples were stored in a 4 °C refrigerator and were analysed for Hg concentration within a week.

The data of throughfall, open field precipitation, and surface and underground runoff depth in Chenqi catchment were obtained from the Puding Karst Ecosystem Research Station, Chinese Academy of Sciences. We quantified throughfall and open field precipitation in Huilong catchment using a rain bucket ($\varphi = 200$ mm, TZZT Co., Ltd.) and the surface and underground runoff depth using a Parshall flume (Green Co., Ltd.).

2.2.2. Litterfall sampling

The annual mass of litterfall was estimated by collecting the monthly litterfall using 1 m × 1 m nylon nets hanging 0.3 m above ground (Fig. S1) at 7 and 15 random sites in Huilong and Chenqi catchments, respectively. A polyethylene net was installed within a box to permit water flow through the net while retaining the litterfall. Litterfall was sampled monthly from August 2018 to July 2019, and three months' samples were combined to generate a composite sample which was air-dried, ground, homogenized and analysed.

2.2.3. Total suspended particulate matter (TSP) and air-surface Hg^0 exchange

In this study, Hg concentration of TSP and its deposition rate were used to calculate total particulate-bound Hg deposition flux (Fang et al., 2014). TSP was sampled monthly from August 2018 to July 2019 using a TSP sampler (gas flow rate 100 L min^{-1}, KB-120F, Qingdao jingcheng instrument co. LTD) with a φ 90 mm quartz filter film (Munktell Inc. Sweden). Sampling was collected every 48 h in every non-rainy period. To obtain TSP deposition, TSP was simultaneously collected using a TSP collecting cylinder (30-cm high, 15-cm diameter, Taiheng plastics co. LTD; 100 mL of pure water and 50 mL of ethylene glycol were added), and the deposition velocity of TSP was calculated from the weight of collected TSP (see Fig. S4).

Air-surface Hg^0 exchange flux for the Huilong catchment has been investigated in previous study (Wang et al., 2005). Considering that there have been no significant changes in the topography and land use of the area and no implemented soil pollution remediation projects in the past two decades, we hypothesized that the previously observed air-surface Hg^0 exchange flux represents the current conditions. Previously established values were thus directly used in the present study.

Air-surface Hg^0 exchange flux for the Chenqi catchment was measured over an 8-day period (July 17–24, 2019) using the novel dynamic flux chamber (NDFC) method (Lin et al., 2012; Yuan et al., 2019; Zhu et al., 2015). The NDFC inlet and outlet were connected to a synchronized multiport sampling system (Tekran® Model 1115) using a PTFE tube with 0.25-inch outer diameter connected to an automated ambient air analyser (Tekran® Model 2537 B) for measuring the ambient air and efflux air Hg concentration, respectively. Flow rates were converted to values under a standard temperature (0 °C) and pressure (101.3 kPa) condition. The Hg flux was calculated as follows:

$$F = \frac{Q}{S} \cdot (C_{out} - C_{in}) \quad (1)$$

where F is Hg flux (ng m^{-2} h^{-1}), Q is the NDFC internal flushing flow rate (m^3 h^{-1}), S is the NDFC flux chamber area (m^2), and C_{out} and C_{in} are Hg concentration at the NDFC outlet and inlet, respectively. In this work, S equals to 0.09 m^2. A positive value for F represents Hg emission from the soil to the atmosphere, while a negative one represents atmospheric Hg deposition to the soil. Parameters such as solar radiation (SR), air temperature and relative humidity (RH) in Chenqi catchment were obtained from the Puding Karst Ecosystem Research Station, Chinese Academy of Sciences.

2.2.4. Crop sampling

Crops were sampled every three months from August 2018 to July 2019. The dominant crops planted in the two catchments were collected. Corn, coix, cabbage, Chinese cabbage and chili were sampled from Huilong, and corn, rice, cabbage and chili were sampled from Chenqi. Crop samples were washed with tap water, and then rinsed with deionized water. The weight of fresh vegetables was recorded to express the data on a wet weight basis. All crop samples were stored at −18 °C prior to being freeze dried using a lyophilizer (EYELA FDU-2110, Tokyo Physical and Chemical Equipment Co., Ltd. Japan) operated at −80 °C and 3 Pa for 72 h. Freeze dried samples were crushed into powder by an electronic grinder (Lixin Laboratory Instrumentation Co., Ltd. Hebei, China). The annual crop biomass production was estimated by harvesting crops in three replicate quadrats (1 m × 1 m) at each sampling site and then multiplying quadrat biomass by planted area.

2.2.5. Fertilizer sampling

The annual mass of fertilizer used was quantified through consultation with local farmers. Chemical fertilizer samples and livestock manure samples were collected from farmers in the villages nearby Chenqi and Huilong, stored in individual polyethylene bags, and transported to the laboratory. All visible roots, macro fauna and stones were removed from fertilizer samples before samples were air-dried, homogenized and passed through a 100-mesh nylon sieve for Hg analysis.

2.2.6. Chemical analysis

The total Hg concentration in the TSP filters, fertilizer, litterfall and crops was measured directly using a Lumex RA915+ Hg analyser equipped with a Pyro 915+ pyrolysis attachment by way of thermal decomposition to Hg^0 (Lumex Ltd. Russia), which has a detection limit of 0.05 μg kg^{-1}. The mass of all filters analysed by this method was weighed using a high precision balance (10^{-4} g). Total Hg and dissolved Hg concentrations in the open field precipitation, throughfall, surface runoff and underground runoff samples were analysed by cold vapor atomic fluorescence spectrometry (Tekran® 2500, refer to the USA EPA Method 1631). Particulate Hg (PHg) concentration was calculated as the difference between THg and DHg. Hg concentrations in water samples were analysed according to the USEPA method 1631, which has a detection limit of 0.02 ng L^{-1}.

2.3. Mass balance budget

Five input pathways and four output pathways of Hg transportation were investigated in the current study. The input pathways include throughfall deposition, open field precipitation deposition, litterfall deposition, total particulate-bound Hg deposition and fertilizer input. The output pathways include air-surface Hg^0 exchange, crop harvesting, surface runoff and underground runoff. The Hg transport flux through the two catchments was calculated by multiplying the Hg concentration and the throughfall, open field precipitation/runoff amount (mm yr^{-1}), yield (kg ha^{-1} yr^{-1}) or deposition velocity (cm s^{-1}), respectively. The calculation of the eight pathways except air-surface Hg^0 exchange can be described as follows:

$$F_{ij} = \sum_k C_{ij} \times E_{ij} \times P_{jk} \quad (2)$$

where F_{ij} (μg m^{-2} yr^{-1}), C_{ij} (ng L^{-1}, μg g^{-1} or ng m^{-3}) and E_{ij} (mm yr^{-1}, kg ha^{-1} yr^{-1} or cm s^{-1}) are annual Hg flux, annual average Hg concentration and annual exported volume or mass of pathway i in catchment j, respectively; and P_{jk} is the proportion of type k utilization land area to the total area of the catchment (see Table 1). Finally, Hg mass balance was quantified separately for each catchment following the approach described in an earlier study (Feng et al., 2009):

$$Net\ flux = \sum output\ flux - \sum input\ flux \quad (3)$$

2.4. Quality control and data analysis

The average relative standard deviation for the duplicate analyses of Hg was 4.5% and matrix spike recoveries ranged from 93% to 117% (mean = 98%, $n = 6$). The equipment blank for throughfall, open field precipitation and runoff samples for Hg was 0.04 ± 0.01 ng L^{-1} ($n = 6$). The reference materials soil GBW07405 and cabbage GBW10014 were used for the soil and plant analytical quality control, respectively. The measured average Hg concentrations of the reference materials were 0.27 ± 0.09 mg kg^{-1} and 11.5 ± 1.45 μg kg^{-1}, respectively ($n = 6$), which were comparable to the certified values of 0.29 ± 0.04 mg kg^{-1} and 10.9 ± 1.6 μg kg^{-1}. The relative percentage differences of sample replicates for soil and plant were <6% and <9%, respectively. The structural equation model (SEM) was used to quantitatively describe the driving factors related to the impact of the air-surface Hg^0 exchange flux. It is a powerful framework for fitting data and figure out direct/indirect effects in complex processes (Wang et al., 2019). Data analysis was performed with Microsoft Office 2019 (Microsoft Corporation., USA), SPSS 24.0, and Amos 24.0 software (SPSS Inc., USA), and the figures were created using Origin 9.0 (Origin Lab Corporation., USA).

3. Results and discussion

3.1. Mercury in throughfall, open field precipitation and runoff

The annual rainfall in Huilong and Chenqi was 1315.5 mm and 1193.6 mm, respectively, and the corresponding throughfall was 723.5 mm and 775.8 mm (Table 1). The ratio of throughfall to open field precipitation in Huilong was 54.9%, slightly lower than that in Chenqi (65.0%), likely due to the higher canopy density and thus higher rainwater retention in the forest of Huilong catchment. The surface and underground runoff was 174.1 mm and 390.2 mm, respectively, in Huilong catchment, and 58.8 mm and 125.4 mm respectively, in Chenqi catchment (Table 1). The greater volumes of underground runoff than surface runoff in both catchments are attributed to the well-developed

Table 1
Annual mass in each input and output pathways and corresponding areas.

	HL	Area (ha)	CQ	Area (ha)
Throughfall (mm)	723.5	15	775.8	120
Open field precipitation (mm)	1315.5	3	1193.6	30
TSP deposit rate (cm s^{-1})	0.23	3	0.21	30
Litterfall (kg ha^{-1})	5270	15	4830	120
C-Fertilizer (kg ha^{-1})	900	3	750	30
O-Fertilizer (kg ha^{-1})	1500	3	1200	30
Surface runoff (mm)	174.1	18	58.8	150
Underground runoff (mm)	390.2	18	125.4	150
Corn seed (kg ha^{-1})	4500	0.9	5250	6
Corn straw (kg ha^{-1})	20,250	0.9	23,625	6
Rice seed (kg ha^{-1})	0	0	7500	18
Rice straw (kg ha^{-1})	0	0	3750	18
Coix seed (kg ha^{-1})	3000	1.5	0	0
Coix straw (kg ha^{-1})	6750	1.5	0	0
Vegetables (kg ha^{-1})	24,132	0.6	31,562	6

underground karst caves and abundant surface fractures in the karst area (Auler and Smart, 2003).

Mercury concentrations in throughfall, open field precipitation, surface runoff and underground runoff in Huilong catchment were 15.4–55.9 ng L^{-1} (mean = 29.4 ± 18.9 ng L^{-1}), 7.9–26.0 ng L^{-1} (mean = 14.5 ± 9.0 ng L^{-1}), 43.5–72.0 ng L^{-1} (mean = 63.9 ± 13.7 ng L^{-1}) and 20.3–34.1 ng L^{-1} (mean = 27.5 ± 6.1 ng L^{-1}), respectively, and in Chenqi catchment were 9.6–45.3 ng L^{-1} (mean = 23.0 ± 16.2 ng L^{-1}), 4.7–21.6 ng L^{-1} (mean = 11.1 ± 7.6 ng L^{-1}), 6.3–16.0 ng L^{-1} (mean = 11.7 ± 4.9 ng L^{-1}) and 9.8–11.2 ng L^{-1} (mean = 10.6 ± 0.57 ng L^{-1}), respectively. The Hg concentrations in throughfall, open field precipitation, surface runoff and underground runoff in Huilong were 0.28 to 4.46-fold higher than those in Chenqi catchment, and this could be attributed to the higher Hg concentration in the various media (air, soil, canopy) in Huilong catchment. There is a mineralised Hg-Tl-As deposit only 2 km away from the Huilong catchment, which had been extensively mined up until 1970 (Jia et al., 2013). Chenqi catchment, on the other hand, is representative of background karst regional geology with no history of Hg mining within 50 km of the site. However, despite being a control catchment, the Hg concentration in the surface soil of Chenqi, was still 3–5 times higher than those in the other areas of China (Nie et al., 2019), and this may explain the much higher Hg concentrations in throughfall, open field precipitation and runoff in Chenqi than those reported for the forest catchments (Larssen et al., 2008; Ma et al., 2016).

Mercury concentrations in throughfall and open field precipitation showed significant seasonal variations with lower values in the rainy season than dry season, likely due to dilution effect of higher precipitation in the rainy season (Kumar et al., 2016; Mayer and Ulrich, 1977). Mercury concentrations in the surface runoff (total Hg = 63.9 ± 13.7 ng L^{-1}) in Huilong catchment were higher than those in the Chenqi catchment (total Hg = 11.7 ± 4.9 ng L^{-1}), which may be attributed to the higher concentration of soil Hg in Huilong catchment (total Hg = 0.41 to 610 mg kg^{-1}) (Qiu et al., 2006), as runoff can carry soil particles containing Hg (Beliveau et al., 2017; Liu et al., 2018). Furthermore, most Hg was identified as particulate-bound Hg both in the surface (64%–89%) and underground runoff (57%–64%), suggesting an important role of particles in migration of Hg in the two catchments. The vertical movement of runoff through the pore fissure structure leads to the formation of underground runoff. The ratios of Hg concentration in the surface runoff to that in the underground runoff were significantly different between the two catchments. We observed lower concentrations of Hg in the underground runoff (THg = 27.5 ± 6.1 ng L^{-1}) than surface runoff (THg = 63.9 ± 13.7 ng L^{-1}) in Huilong catchment. This phenomenon may be a function of Hg precipitation and effective removal from runoff in underground caves that decreased the concentration of particle-bound Hg. In contrast, there was no clear reduction of Hg in the underground runoff as compared to the surface runoff in Chenqi catchment, and this may be attributed to the lower prevalence of caves in this catchment.

Mercury concentrations in throughfall and open field precipitation in Huilong catchment were 15.4–55.9 ng L^{-1} (mean = 29.4 ± 18.9 ng L^{-1}) and 7.9–26.0 ng L^{-1} (mean = 14.5 ± 9.0 ng L^{-1}), respectively, and in Chenqi catchment were 9.6–45.3 ng L^{-1} (mean = 23.0 ± 16.2 ng L^{-1}) and 4.7–21.6 ng L^{-1} (mean = 11.1 ± 7.6 ng L^{-1}), respectively (Fig. 2). The concentrations of Hg both in throughfall and open field precipitation showed a seasonal variation with order of Nov-Jan > Feb-Apr > Aug-Oct > May-Jul. High Hg concentrations observed between November and January might be caused by intensive fossil fuel/biomass combustion, superimposed by limited wet scavenging due to small amounts of precipitation during this period (Obrist et al., 2008; Seo et al., 2012).

Particulate Hg also strongly correlated with THg in the throughfall samples ($R = 0.71$ and 0.86, $p < 0.05$) and open field precipitation samples ($R = 0.43$ and 0.72, $p < 0.01$) in Huilong and Chenqi catchment, respectively (Fig. 3). The corresponding percentage of THg as PHg was 54%

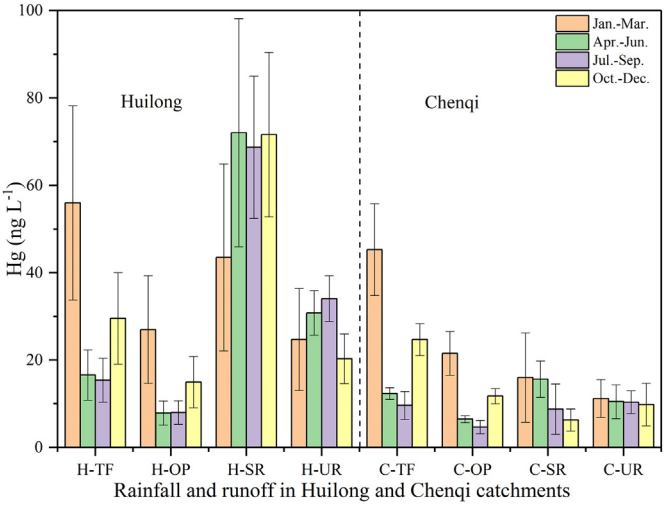

Fig. 2. Mercury concentrations in throughfall (TF), open field precipitation (OP), surface runoff (SR) and underground runoff (UR) in Huilong catchment (H-TF, H-OP, H-SR and H-UR) and Chenqi catchment (C-TF, C-OP, C-SR and C-UR). Error bars represent confidence intervals.

and 51% in throughfall samples and 39% and 47% in open field precipitation samples. The above contrasting trends in the PHg to THg ratio between the two catchments were likely caused by their different canopy types and densities (Demers et al., 2007; Witt et al., 2009). Huilong catchment is dominated by coniferous forest (Taxodiaceae Warming) while Chenqi catchment by deciduous forest (*Catalpa fargesii Bur. f. duclouxii (Dode) Gilmour, Camptotheca acuminata Decne*, etc.). The removal efficiency of Hg has been reported to be higher in coniferous than deciduous forests due to larger specific surface areas of coniferous trees, which can accumulate more PHg from air and thus enhance Hg in throughfall (Fisher and Wolfe, 2012; Wright et al., 2016).

Particulate Hg also strongly correlated with THg in the surface runoff samples ($R = 0.89$ and 0.91, $p < 0.05$) and underground runoff samples ($R = 0.83$ and 0.74, $p < 0.05$) in Huilong and Chenqi catchment, respectively, and the corresponding average ratios of PHg to THg were 64% and 89% in surface runoff samples and 57% and 64% in underground runoff samples. These high ratios indicate that PHg is the dominant fraction of THg in surface and underground runoff, suggesting the important role particles played in Hg movement in the two catchments (Amirbahman et al., 2002). Particles with high organic matter are known to be more abundant in surface water than in deep groundwater, and such particles may be the main carrier of Hg in the two catchments (Aastrup et al., 1991; Zhou et al., 2017). For example, an earlier study reported that the amount of particulate matter and Hg in the runoff during a summer storm event were 70-fold and 20-fold higher than those during normal periods in an agricultural basin (Babiarz et al., 1998). It was also reported that about 60% to 75% of Hg exported in another basin was in the form of particulate matter during high-flow periods every year (Scherbatskoy et al., 1998; Vermilyea et al., 2017). In previous studies Hg has been shown to be mainly associated with particulate organic carbon (POC), as indicated by a positive correlation between particulate Hg and POC (Canario et al., 2007; Covelli et al., 2006). POC plays an important role in promoting the transport of Hg in catchment water systems. (Häggi et al., 2019; Kolka et al., 1999; Lim et al., 2019).

3.2. Mercury in TSP deposition and litterfall

Air concentrations of Hg in TSP were 270–710 pg m^{-3} (mean = 520 pg m^{-3}, $n = 12$) and 170–330 pg m^{-3} (mean = 230 pg m^{-3}, n = 12) and those of the atmospheric Hg^0 were 35.2–111.2 ng m^{-3} (Wang et al., 2005) and 2.13–3.05 ng m^{-3} in Huilong and Chenqi catchments, respectively (Fig. 4)). The percentage of total atmospheric Hg

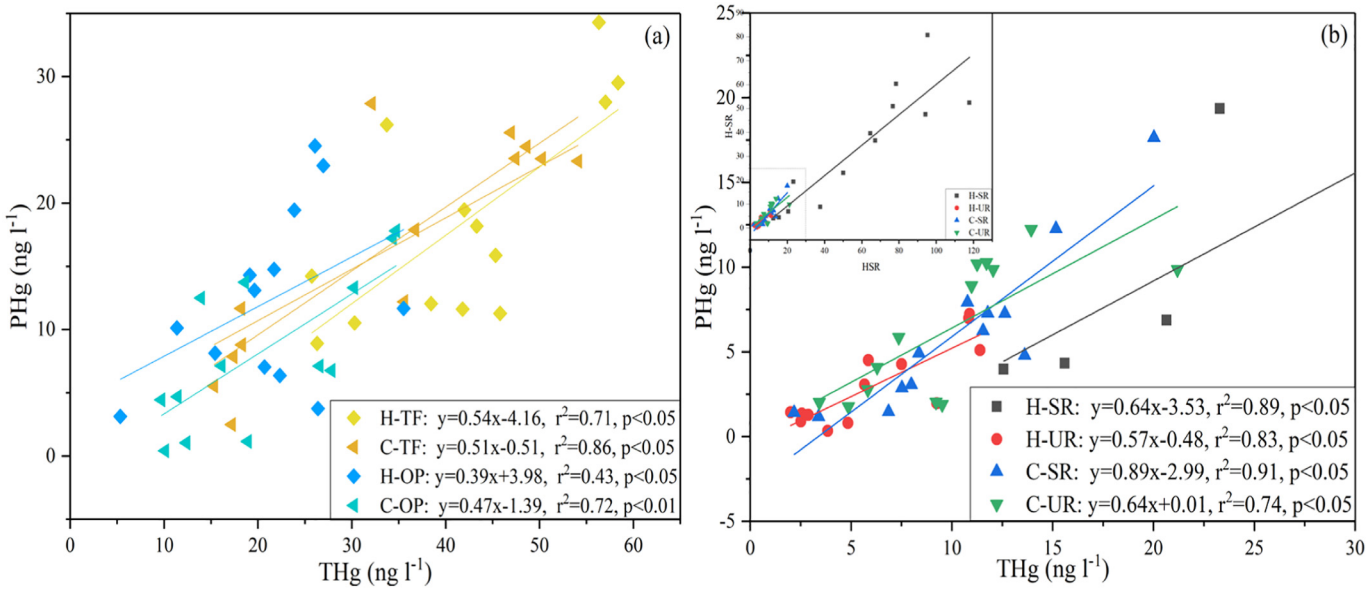

Fig. 3. Linear correlation between THg and PHg in (a) throughfall and open field precipitation and (b) surface runoff and underground runoff in Huilong and Chenqi catchments. Throughfall (TF), open field precipitation (OP), surface runoff (SR) and underground runoff (UR) in Huilong catchment (H-TF, H-OP, H-SR and H-UR) and Chenqi catchment (C-TF, C-OP, C-SR and C-UR).

(the sum of TSP Hg and Hg^0) as TSP Hg was 0.63%–0.76% and 6.4%–11.8% in Huilong and Chenqi catchments, respectively. The much higher ratios in Chenqi than Huilong were likely because Chenqi was affected by more anthropogenic sources due to its vicinity to a city (Puding). A previous study showed that the proportion of TSP Hg in THg was particularly high in Chinese urban areas (5.2–17.2%), when compared with the overall average of all available measurements (2.5%) (Zhang et al., 2015).

Mercury concentrations in litterfall were in the range of 0.14–0.52 μg g^{-1} (mean = 0.29 μg g^{-1}, n = 84) and 0.046–0.083 μg g^{-1} (mean = 0.065 μg g^{-1}, n = 180) in Huilong and Chenqi catchments, respectively. The generally higher litterfall Hg concentration in Huilong than Chenqi catchment was likely due to the higher background level of Hg in the Huilong catchment. The high geological background of Hg in this catchment resulted in high soil Hg concentrations, which in turn led to high soil emissions of Hg^0 to the atmosphere (Juillerat and Ross, 2010; Juillerat et al., 2012) and high accumulation of Hg^0 by the foliage of plants (Laacouri et al., 2013; Zhang et al., 2016).

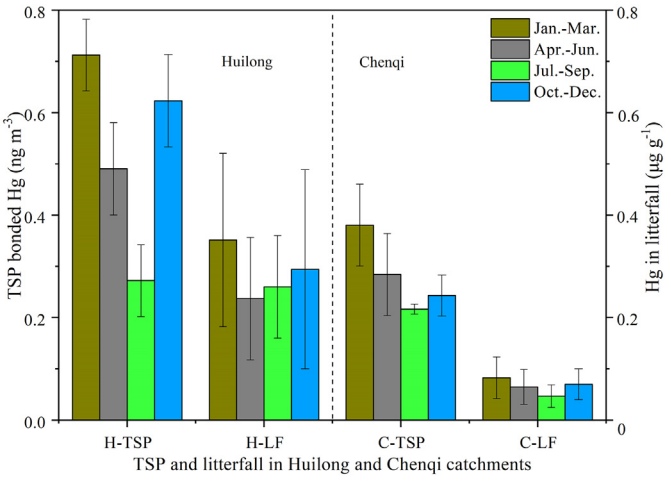

Fig. 4. Air concentrations of Hg in total suspended particles (TSP) and litterfall (LF) in Huilong (H-TSP and H-LF) and Chenqi (C-TSP and C-LF) catchments. Error bars represent confidence intervals.

3.3. Air-surface Hg^0 exchange

The daily changes in atmospheric Hg concentration at the inlet/outlet end of the Hg exchange flux tank, Hg exchange flux, light intensity, atmospheric humidity and temperature in the Chenqi catchment are presented in Fig. 5. Among these variables, apparent diurnal variations were seen in the atmospheric Hg concentration at the outlet end of the Hg exchange flux box, the Hg exchange flux, the light intensity and the temperature, with significantly increased values during the time period of 10:00–17:00. However, such variations were not seen in the atmospheric Hg concentration and atmospheric humidity at the intake end of the Hg exchange flux box. The measured atmospheric Hg concentration was 2.47 ± 0.25 ng m^{-3} and the air-surface Hg^0 exchange flux at 9.79 ± 3.38 ng m^{-2} h^{-1}. The structural equation model (SEM) analysis suggests that solar radiation (SR) (40.9%) and temperature (39.1%) were the two dominant factors driving air-surface Hg^0 exchange. A significant linear correlation between the average Hg flux and average SR and temperature was obtained as follows:

$$F = (0.022 \pm 0.004) \times S + (0.85 \pm 0.24) \times T - 10.87, R^2 = 0.77 \quad (4)$$

where F is Hg flux (ng m^{-2} h^{-1}), S is SR (W m^{-2}), and T is air temperature (°C).

The annual air-surface Hg^0 exchange flux was roughly estimated using Eq. (4) with annual average solar radiation (98.58 W m^{-2}) and temperature (15.1 °C) as input, which produced a flux of 36.2 ± 48.5 μg m^{-2} yr^{-1} in Chenqi catchment. The annual flux in Chenqi, although 30 times lower than that (1226 ± 1307 μg m^{-2} yr^{-1}) previously reported for the Huilong catchment (Wang et al., 2005), was still 5 times higher than that observed at the Ailao mountain (a background region) (Zhou et al., 2019; Zhu et al., 2016), likely because the forest densities in karst areas are much smaller than those in the other forests.

3.4. Hg in crops and fertilizer

The Hg concentrations in different crops and plant parts harvested from Huilong catchment ranged from 0.019 to 0.32 μg g^{-1}, with the lowest value in corn grain and the highest in corn stem and leaf (Fig. S6). The Hg concentrations in plants from Chenqi catchment ranged from 0.007 to 0.064 μg g^{-1}, with the lowest value in corn grain

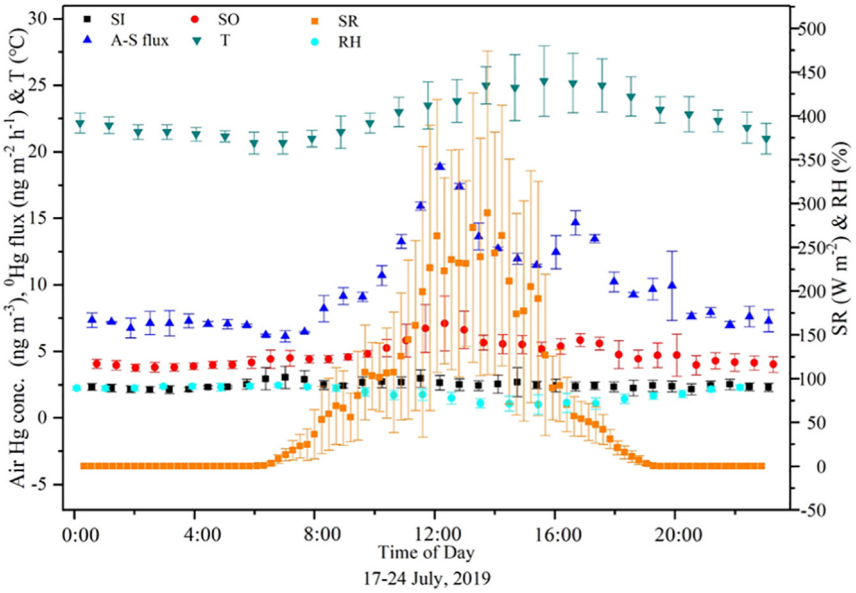

Fig. 5. Diurnal variations of air-surface Hg^0 fluxes and meteorological parameters. SI and SO are the atmospheric Hg concentrations in the inlet and outlet of the flux chamber, respectively. SR, A-S flux, T and RH are solar radiation, air-surface Hg^0 exchange flux, air temperature and relative humidity, respectively. Error bars denote one standard deviation (1SD) of the mean.

and the highest value in rice stem and leaf (Fig. 6). The Hg concentrations in agricultural products across Huilong were significantly higher than the Chinese governmental reference value for Hg in food crops (10–20 μg kg^{-1}, fresh weight). The primary source of Hg accumulated in the above-ground plant parts is Hg in the atmosphere (Cui et al., 2014; Manceau et al., 2018). Plant uptake of Hg from soil to plant roots and into aerial portions varies between crop species but is generally limited, and is controlled by soil chemical properties such as soil organic matter and soil pH (Hlodak et al., 2014). The magnitude of Hg removal through crop (straw) harvesting depends on the yield of the crop and the area sown (Shi et al., 2019). According to the farming habits of local farmers, crop straw was mostly recycled by farmers for feeding animals or heating purpose.

The average Hg concentrations in chemical fertilizers applied to farmland in Huilong and Chenqi catchments were 0.76 ± 0.20 μg g^{-1} and 0.81 ± 0.17 μg g^{-1}, respectively, and those of livestock manure used in these two catchments were 0.98 ± 0.19 μg g^{-1} and 0.47 ± 0.17 μg g^{-1}, respectively. Fertilization accounted for 13.4% and 24.5% of the total Hg input flux in Huilong and Chenqi catchment, respectively (Fig. 6), of which 68.2% and 48.1%, respectively, were from livestock manure. Successive years of chemical fertilizer and livestock manure application have contributed to the accumulation of Hg in the cultivated topsoil (Liu et al., 2012). In agreement with a previous study, the dominant vector for imported Hg is livestock waste (average 50.25%) (Shi et al., 2019).

3.5. Characteristics of mercury mass balance in the two catchments

Input and output Hg fluxes from individual pathways were estimated by combining the annual mass of Hg associated with each pathway and the corresponding area (Table 1). The estimated input Hg fluxes associated with throughfall, open field precipitation, litterfall, particulate-bound Hg deposition and fertilizer application were 17.7 ± 11.4, 3.2 ± 1.9, 129 ± 85.3, 33.1 ± 12.1 and 28.4 ± 19.4 μg m^{-2} yr^{-1}, respectively, in Huilong catchment, and were 14.2 ± 10.1, 2.6 ± 1.8, 25.0 ± 15.6, 15.2 ± 5.23 and 18.5 ± 10.2 μg m^{-2} yr^{-1}, respectively, in Chenqi catchment. The estimated output fluxes associated with air-surface Hg^0 exchange, crops harvesting, surface runoff and underground runoff were 1226 ± 1307, 462 ± 66.4, 11.0 ± 0.48 and 10.6 ± 0.45 μg m^{-2} yr^{-1}, respectively, in Huilong catchment, and were 36.2 ± 48.5, 43.0 ± 6.29, 0.74 ± 0.15 and 1.31 ± 0.30 μg m^{-2} yr^{-1}, respectively, in Chenqi catchment. From the above numbers the net Hg fluxes were calculated as 1498.2 ± 1504 μg m^{-2} yr^{-1} and 4.8 ± 98.2 μg m^{-2} yr^{-1} in Huilong and Chenqi catchments, respectively. The large negative value in Huilong catchment suggests that it as a significant source of Hg to the karst ecosystem, while the small (close to zero) value for Chenqi suggests it as a minor source, if not sink of Hg (Fig. 6).

Many studies have reported forests or farmlands as Hg sinks (Table 2), which contrasts markedly with the results of the present study, especially for the farmland forestland karst catchments in Huilong. The high geological background Hg concentration in this region is likely to be a major cause for these catchments being a net source of Hg. The net flux of Hg through air-surface Hg^0 exchange was significantly higher in our study areas than in other regions with low levels of geological background Hg. However, natural flux may be amplified by the current agricultural land use which leads to significant Hg output in crops. The output/input Hg mass ratios recorded in this study were significantly higher than those for the other forest and agricultural ecosystems (Table 2), and two-fold higher than values reported for the Wanshan Hg mining area, which has previously been described as a case study for Hg pollution.

Mercury mass balance discussed above revealed that Huilong catchment appears to be a distinct Hg source, while Chenqi catchment is a possible Hg source. The main input pathways of Hg in the Huilong catchment are litterfall and TSP deposition, which together account for 76.7% of the total input flux. The input fluxes of these two pathways in Huilong catchment are 5.2 and 2.2 times, respectively, of those in the Chenqi catchment, indicating lower environmental quality in terms of atmospheric Hg in Huilong than Chenqi catchment. For areas with high geological background Hg, litterfall dominates the fate of atmospheric Hg to soil, such as the case in Huilong catchment. Input Hg fluxes from open field precipitation and throughfall were slightly larger in Huilong than Chenqi catchment, likely due to the higher atmospheric Hg concentration and denser canopy in Huilong. The dry deposition of Hg occupies a dominant position in all input pathways in the study areas. The atmospheric Hg dry/wet deposition ratios are 55.1 and 19.9 in Huilong and Chenqi, respectively. Fertilization input also played an important role in the Hg input of both catchments.

The largest output pathway of Hg in Huilong catchment was the process of air-surface Hg^0 exchange, suggesting that the release of soil Hg to the atmosphere plays a critical role in the environmental quality of local

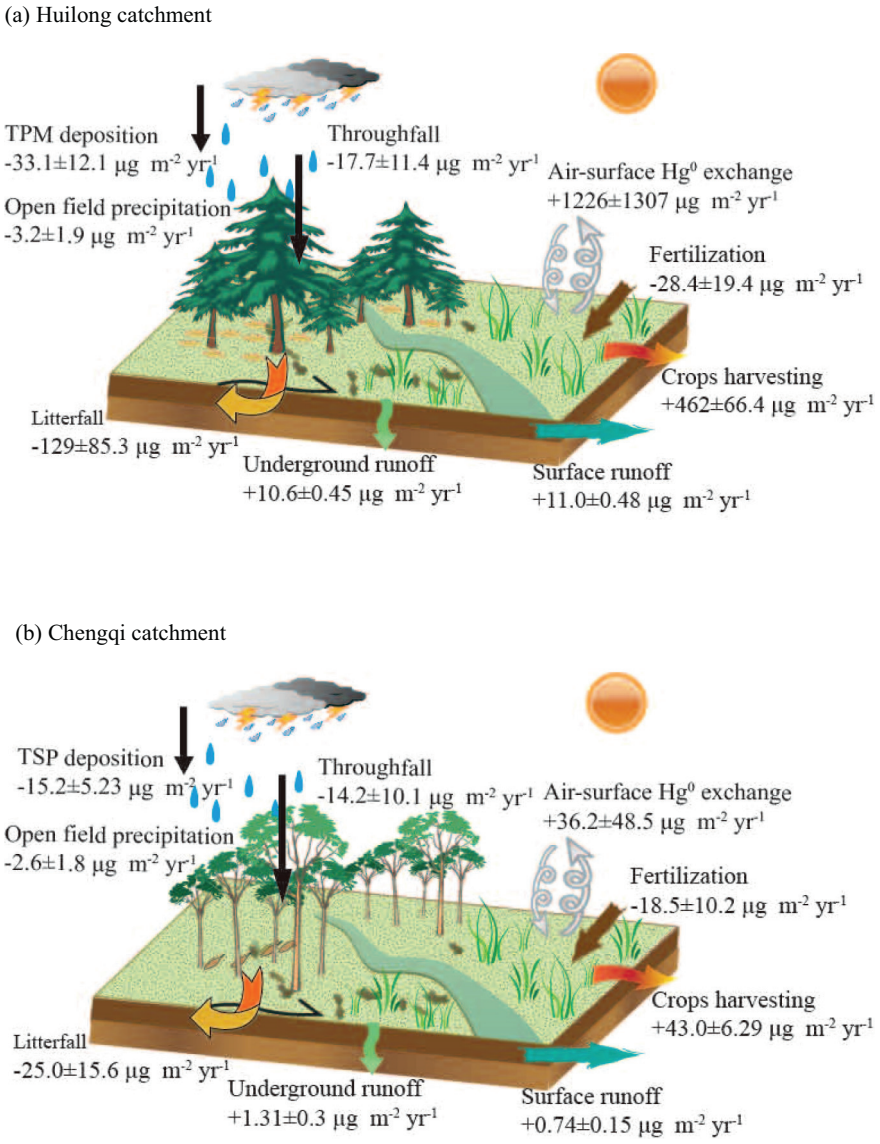

Fig. 6. Schematic illustration of mass balance of Hg in Huilong and Chenqi catchments. "-" means Hg input flux, and "+" means Hg output flux.

atmospheric Hg in areas with high Hg geological background. Even in Chenqi catchment, the contribution of air-surface Hg^0 exchange ranked the second largest of the four output pathways. The output Hg flux through crop harvest is much higher in Huilong than Chenqi catchment due to the much higher Hg concentration in crops in Huilong catchment. Such a finding implies that local residents in Huilong are at a greater level risk of Hg exposure than those in Chenqi. In the Chenqi catchment, crop harvest is ranked the first of all output pathways. The Hg fluxes through surface runoff and underground runoff in Huilong catchment are both about 10 times of those in Chenqi catchment, revealing that considerable amounts of Hg were diffused into the surrounding environment through runoff, especially in Huilong. Moreover, it was found that the Hg fluxes from underground runoff were close to or even higher than those from the surface runoff.

Table 2
Annual Hg flux in this study and literature (μg m^{-2} yr^{-1}).

Study sites	Types	Throughfall/ irrigation	Litterfall	TSP deposition	Fertilizer	Air-surface Hg^0 exchange	Crops harvesting	Runoff	Net flux	Ratio of output/input	References
Wanshan, China	Mining area	593	/	6178	/	3967	10.4	3020	226.4	1.033	(Dai et al., 2012; Wang et al., 2007)
Langtjern, Norway	Boreal forest	6.7	2.7	/	/	/	/	2.5	−4.5	0.266	(Larssen et al., 2008)
Serra do Navio, Brazil	Tropical forest	18.2	/	54.0	/	/	/	2.9	−69.1	0.040	(Fostier et al., 2000)
Mt. Jinyun, China	Subtropical forest	17.1	49.8	/	/	62.6	/	1.9	−13.8	0.964	(Sun et al., 2019)
Taizhou, China	Agro-ecosystem	136	/	20	375	/	67	71	−393	0.260	(Shi et al., 2019)
Nanjing, China	Agro-ecosystem	33.0	/	19.2	2.9	/	5.6	2.5	−23	0.147	(Hou et al., 2014)
Mt. Simian, China	Subtropical forest	32.2	42.9	/	/	18.6	/	7.2	−49.3	0.343	(Ma et al., 2016)
Huilong, China	Karst-ecosystem	19.1	129	33.1	28.4	1226	462	21.6	1498.2	8.157	This study
Chenqin, China	Karst-ecosystem	6.3	25.0	15.2	18.5	85.8	43.0	2.0	4.8	2.012	This study

The ecological drivers played important roles in Hg biogeochemical cycling in karst ecosystems. The vegetation types and density affect the throughfall Hg input efficiency. For example, forest types in Huilong is mainly coniferous forest, while in Chenqi is coniferous-broadleaf mixed forest and the density of trees is higher in Huilong than Chenqi, which led to higher scour efficiency and more Hg in throughfall in Huilong. Hence the rainwater from the Huilong scour the forest canopy more efficiently and carry out more Hg. Forest cover was beneficial to the increase of soil organic matter in the forestland surface, which contributed to the complexity of soil Hg and reduced its mobility (Jiskra et al., 2014; Leff et al., 2012). Increasing forest cover has important positive effect on controlling the risk of Hg pollution and soil erosion in karst areas with high Hg background. It is noted that Huilong catchment is located in the Hg mine area, while Chenqi is not, thus, the very different Hg geological background in these two catchments results in their significantly different input/output pathways in Hg mass balance and intensities as Hg sources.

The high Hg geological background provides the necessary Hg source for the development of high soil Hg concentration, which in turn lead to high ambient Hg concentration. In contrast, the low Hg geological background governs the intensity of the migration and transmission of relatively low Hg in natural processes in karst catchment systems. Therefore, attention should be paid to the possibility of elevated Hg concentrations in groundwater in karst areas with high geological background Hg. For the control and abatement of Hg pollution in Huilong catchment, Hg migration and diffusion to the atmosphere and water bodies, especially to groundwater, should be considered together. Data from this investigation suggests that the karst farmland-forest ecosystem in southwest China is a key contributor to regional Hg emissions, and more research are needed to assess the impact of different land use types on the emission of Hg from soil to the atmosphere.

4. Conclusions and implications

This work investigated the mass flow intensities of various input and output pathways of Hg and calculated the mass balance of Hg in two karst catchments. Natural factors, such as litterfall input and air-surface Hg^0 exchange dominated Hg flux, while human factors, such as fertilizer input and Hg removal through crop harvesting, also significantly impacted Hg mass balance in both catchments. The Hg geological background is the critical factor to drive the Hg geochemistry cycling in karst region.

Mercury released from the karst area into the atmosphere would migrate to the surrounding environment through air-surface Hg^0 exchange, runoff and crop harvesting, causing potential Hg exposure to local residents. Using low-Hg fertilizers, reducing livestock manure application, and changing land use by planting crops with low-Hg accumulation capacity should be considered in the future to reduce Hg pollution in vulnerable karst areas, especially in areas with high Hg geological background. Future policies should also be established to protect the fragile karst ecosystems of southwest China. Policies could promote improved farm management practices and increased vegetation cover in order to reduce the adverse environmental and health impacts of Hg diffusion from this high-Hg geological region.

CRediT authorship contribution statement

Jicheng Xia: Investigation, Methodology, Data curation, Formal analysis, Writing – original draft, Writing – review & editing. **Jianxu Wang:** Investigation, Data curation, Conceptualization, Writing – review & editing. **Leiming Zhang:** Conceptualization, Writing – review & editing. **Xun Wang:** Formal analysis, Investigation, Writing – review & editing. **Wei Yuan:** Investigation, Data curation, Conceptualization. **Christopher W.N. Anderson:** Conceptualization, Writing – review & editing. **Chaoyue Chen:** Methodology, Investigation. **Tao Peng:** Methodology, Investigation. **Xinbin Feng:** Supervision, Conceptualization, Methodology, Formal analysis, Writing – review & editing.

Declaration of competing interest

The authors declare that they have no known competing financialinterestsor personal relationships that could have appeared to influence the work reported in this paper.

Acknowledgments

This work is supported by the Program Foundation of Institute for Scientific Research of Karst Area of NSFC-GZGOV [U1612442], the National Key R&D Program of China [2017YFD0800302] and the Strategic Priority Research Program of Chinese Academy of Sciences [XDB40000000]. Constructive comments from Prof. Bo Meng of Institute of Geochemistry (CAS) are greatly appreciated.

Appendix A. Supplementary data

Supplementary data to this article can be found online at https://doi.org/10.1016/j.scitotenv.2020.144892.

References

Aastrup, M., Johnson, J., Bringmark, E., Bringmark, L., Iverfeldt, A., 1991. Occurrence and transport of mercury within a small catchment-area. Water Air Soil Poll 56, 155–167.
Amirbahman, A., Reid, A.L., Haines, T.A., Kahl, J.S., Arnold, C., 2002. Association of methylmercury with dissolved humic acids. Environ Sci Technol 36, 690–695.
Auler, A.S., Smart, P.L., 2003. The influence of bedrock-derived acidity in the development of surface and underground karst: evidence from the precambrian carbonates of semi-arid northeastern Brazil. Earth Surf. Process. Landf. 28, 157–168.
Babiarz, C.L., Hurley, J.P., Benoit, J.M., Shafer, M.M., Andren, A.W., Webb, D.A., 1998. Seasonal influences on partitioning and transport of total and methylmercury in rivers from contrasting watersheds. Biogeochemistry 41, 237–257.
Barkay, T., Wagner-Dobler, I., 2005. Microbial transformations of mercury: potentials, challenges, and achievements in controlling mercury toxicity in the environment. Adv. Appl. Microbiol. 57, 1–52.
Beliveau, A., Lucotte, M., Davidson, R., Paquet, S., Mertens, F., Passos, C.J., et al., 2017. Reduction of soil erosion and mercury losses in agroforestry systems compared to forests and cultivated fields in the brazilian amazon. J. Environ. Manag. 203, 522–532.
Canario, J., Prego, R., Vale, C., Branco, V., 2007. Distribution of mercury and monomethylmercury in sediments of vigo ria, nw iberian peninsula. Water Air Soil Poll 182, 21–29.
Ci, Z.J., Zhang, X.S., Wang, Z.W., Wang, C.J., 2014. Mass balance of mercury for the yellow sea downwind and downstream of east asia: the preliminary results, uncertainties and future research priorities. Biogeochemistry 118, 243–255.
Covelli, S., Piani, R., Kotnik, J., Horvat, M., Faganeli, J., Brambati, A., 2006. Behaviour of hg species in a microtidal deltaic system: the isonzo river mouth (northern adriatic sea). Sci. Total Environ. 368, 210–223.
Cui, L., Feng, X., Lin, C.-J., Wang, X., Meng, B., Wang, X., et al., 2014. Accumulation and translocation of (198)hg in four crop species. Environ. Toxicol. Chem. 33, 334–340.
Dai, Z.H., Feng, X.B., Fu, X.W., Li, P., 2012. Spatial distribution of mercury deposition fluxes in wanshan hg mining area, Guizhou, China. Atmospheric Chemistry and Physics Discussions 12, 5739–5769.
Demers, J.D., Driscoll, C.T., Fahey, T.J., Yavitt, J.B., 2007. Mercury cycling in litter and soil in different forest types in the adirondack region, New York, USA. Ecol. Appl. 17, 1341–1351.
Fang, Lin Y.H., Chang, C.Y., Zheng, Y.C., 2014. Concentrations of particulates in ambient air, gaseous elementary mercury (gem), and particulate-bound mercury (hg(p)) at a traffic sampling site: a study of dry deposition in daytime and nighttime. Environ Geochem Hlth 36, 605–612.
Feng, X.B., Jiang, H.M., Qiu, G.L., Yan, H.Y., Li, G.H., Li, Z.G., 2009. Mercury mass balance study in wujiangdu and dongfeng reservoirs, Guizhou, China. Environ. Pollut. 157, 2594–2603.
Fisher, L.S., Wolfe, M.H., 2012. Examination of mercury inputs by throughfall and litterfall in the great smoky mountains national park. Atmos. Environ. 47, 554–559.
Fostier, A.H., Forti, M.C., Guimaraes, J.R.D., Melfi, A.J., Boulet, R., Santo, C.M.E., et al., 2000. Mercury fluxes in a natural forested amazonian catchment (serra do navio, amapa state, brazil). Sci. Total Environ. 260, 201–211.
Gao, N., Armatas, N.G., Shanley, J.B., Kamman, N.C., Miller, E.K., Keeler, G.J., et al., 2006. Mass balance assessment for mercury in lake champlain. Environ Sci Technol 40, 82–89.
Häggi, C., Schefuß, E., Sawakuchi, A.O., Chiessi, C.M., Mulitza, S., Bertassoli, D.J., et al., 2019. Modern and late pleistocene particulate organic carbon transport by the amazon river: insights from long-chain alkyl diols. Geochim Cosmochim Ac 262, 1–19.
Hlodak, M., Matus, P., Urik, M., 2014. Mercury geochemistry and analytical methods of determination and fractionation of mercury in soils and plants. Chem. List. 108, 1119–1124.

Hong, Y.S., Hull, P., Rifkin, E., Bouwer, E.J., 2013. Bioaccumulation and biomagnification of mercury and selenium in the Sarasota bay ecosystem. Environ. Toxicol. Chem. 32, 1143–1152.
Hou, Q.Y., Yang, Z.F., Ji, J.F., Yu, T., Chen, G.G., Li, J., et al., 2014. Annual net input fluxes of heavy metals of the agro-ecosystem in the yangtze river delta, China. J. Geochem. Explor. 139, 68–84.
Huang, Q.H., Cai, Y.L., Xing, X.S., 2008. Rocky desertification, antidesertification, and sustainable development in the karst mountain region of Southwest China. Ambio 37, 390–392.
Jia, Y.L., Xiao, T.F., Zhou, G.Z., Ning, Z.P., 2013. Thallium at the interface of soil and green cabbage (brassica oleracea l. Var. Capitata l.): soil-plant transfer and influencing factors. Sci. Total Environ. 450, 140–147.
Jiang, Lian, Y.Q., Qin, X.Q., 2014. Rocky desertification in Southwest China: impacts, causes, and restoration. Earth-Sci. Rev. 132, 1–12.
Jiskra, M., Saile, D., Wiederhold, J.G., Bourdon, B., Bjorn, E., Kretzschmar, R., 2014. Kinetics of hg(ii) exchange between organic ligands, goethite, and natural organic matter studied with an enriched stable isotope approach. Environ Sci Technol 48, 13207–13217.
Juillerat, J.I., Ross, D.S., 2010. Mercury deposition through litterfall and subsequent accumulation in soils: does forest community type matter? Geochim. Cosmochim. Ac 74, A484-A484.
Juillerat, J.I., Ross, D.S., Bank MS, 2012. Mercury in litterfall and upper soil horizons in forested ecosystems in Vermont, USA. Environ. Toxicol. Chem. 31, 1720–1729.
Kolka, R.K., Grigal, D.F., Verry, E.S., Nater, E.A., 1999. Mercury and organic carbon relationships in streams draining forested upland peatland watersheds. J. Environ. Qual. 28, 766–775.
Kumar, S., Siingh, D., Singh, R.P., Singh, A.K., 2016. The influence of meteorological parameters and atmospheric pollutants on lightning, rainfall, and normalized difference vegetation index in the indo-gangetic plain. Int. J. Remote Sens. 37, 53–77.
Laacouri, A., Nater, E.A., Kolka, R.K., 2013. Distribution and uptake dynamics of mercury in leaves of common deciduous tree species in Minnesota, U.S.A. Environ Sci Technol 47, 10462–10470.
Larssen, T., de Wit, H.A., Wiker, M., Halse, K., 2008. Mercury budget of a small forested boreal catchment in southeast Norway. Sci. Total Environ. 404, 290–296.
Leff, J.W., Wieder, W.R., Taylor, P.G., Townsend, A.R., Nemergut, D.R., Grandy, A.S., et al., 2012. Experimental litterfall manipulation drives large and rapid changes in soil carbon cycling in a wet tropical forest. Glob. Chang. Biol. 18, 2969–2979.
Lessard, C.R., Poulain, A.J., Ridal, J.J., Blais, J.M., 2013. Steady-state mass balance model for mercury in the st. Lawrence river near Cornwall, Ontario, Canada. Environ. Pollut. 174, 229–235.
Li, P., Feng, X., Qiu, G., Shang, L., Wang, S., 2012. Mercury pollution in Wuchuan mercury mining area, Guizhou, southwestern China: the impacts from large scale and artisanal mercury mining. Environ. Int. 42, 59–66.
Lim, A.G., Sonke, J.E., Krickov, I.V., Manasypov, R.M., Loiko, S.V., Pokrovsky, O.S., 2019. Enhanced particulate hg export at the permafrost boundary, western siberia. Environ. Pollut. 254, 113083.
Lin, C.J., Zhu, W., Li, X.C., Feng, X.B., Sommar, J., Shang, L.H., 2012. Novel dynamic flux chamber for measuring air-surface exchange of hg-o from soils. Environ Sci Technol 46, 8910–8920.
Liu, Z.A., Yang, J.P., Yang, Z.C., Zou, J.L., 2012. Effects of rainfall and fertilizer types on nitrogen and phosphorus concentrations in surface runoff from subtropical tea fields in Zhejiang, China. Nutr Cycl Agroecosys 93, 297–307.
Liu, M.D., Zhang, Q.R., Luo, Y., Mason, R.P., Ge, S.D., He, Y.P., et al., 2018. Impact of water-induced soil erosion on the terrestrial transport and atmospheric emission of mercury in China. Environ Sci Technol 52, 6945–6956.
Liu, Zhang Q.R., Ge, S.D., Mason, R.P., Luo, Y., He, Y.P., et al., 2019. Rapid increase in the lateral transport of trace elements induced by soil erosion in major karst regions in China. Environ Sci Technol 53, 4206–4214.
Ma, M., Wang, D.Y., Du, H.X., Sun, T., Zhao, Z., Wang, Y.M., et al., 2016. Mercury dynamics and mass balance in a subtropical forest, southwestern China. Atmos. Chem. Phys. 16, 4529–4537.
Macleod, M., Mckone, T.E., Mackay, D., 2005. Mass balance for mercury in the San Francisco bay area. Environ Sci Technol 39, 6721–6729.
Manceau, A., Wang, J., Rovezzi, M., Glatzel, P., Feng, X., 2018. Biogenesis of mercury-sulfur nanoparticles in plant leaves from atmospheric gaseous mercury. Environ Sci Technol 52, 3935–3948.
Mayer, R., Ulrich, B., 1977. Acidity of precipitation as influenced by filtering of atmospheric sulfur and nitrogen-compounds - its role in element balance and effect on soil. Water Air Soil Poll 7, 409–416.
Nelson, S.J., Johnson, K.B., Kahl, J.S., Haines, T.A., Fernandez, I.J., 2007. Mass balances of mercury and nitrogen in burned and unburned forested watersheds at acadia national park, Maine, USA. Environ. Monit. Assess. 126, 69–80.
Nie, L.S., Liu, X.M., Wang, X.Q., Liu, H.L., Wang, W., 2019. Interpretation of regional-scale distribution of high hg in soils of karst area in southwest China. Geochem-Explor Env A 19, 289–298.
Obrist, D., Moosmueller, H., Schuermann, R., Chen, L.W.A., Kreidenweis, S.M., 2008. Particulate-phase and gaseous elemental mercury emissions during biomass combustion: controlling factors and correlation with particulate matter emissions. Environ Sci Technol 42, 721–727.
Qiu, G.L., Feng, X.B., Wang, S.F., Mao, T.F., 2006. Mercury contaminations from historic mining to water, soil and vegetation in lanmuchang, Guizhou, southwestern China. Sci. Total Environ. 368, 56–68.
Scherbatskoy, T., Shanley, J.B., Keeler, G.J., 1998. Factors controlling mercury transport in an upland forested catchment. Water Air Soil Poll 105, 427–438.
Seo, Y.-S., Han, Y.-J., Choi, H.-D., Holsen, T.M., Yi, S.-M., 2012. Characteristics of total mercury (tm) wet deposition: scavenging of atmospheric mercury species. Atmos. Environ. 49, 69–76.
Shi, T.R., Ma, J., Wu, F.Y., Ju, T.N., Gong, Y.W., Zhang, Y.Y., et al., 2019. Mass balance-based inventory of heavy metals inputs to and outputs from agricultural soils in Zhejiang province, China. Sci. Total Environ. 649, 1269–1280.
Sun, J.L., Zou, X., Ning, Z.P., Sun, M., Peng, J.Q., Xiao, T.F., 2012. Culturable microbial groups and thallium-tolerant fungi in soils with high thallium contamination. Sci. Total Environ. 441, 258–264.
Sun, T., Ma, M., Wang, X., Wang, Y., Du, H., Xiang, Y., et al., 2019. Mercury transport, transformation and mass balance on a perspective of hydrological processes in a subtropical forest of China. Environ. Pollut. 254, 113065.
Vermilyea, A.W., Nagorski, S.A., Lamborg, C.H., Hood, E.W., Scott, D., Swarr, G.J., 2017. Continuous proxy measurements reveal large mercury fluxes from glacial and forested watersheds in Alaska. Sci. Total Environ. 599, 145–155.
Wang, S.F., Feng, X.B., Qiu, G.L., Wei, Z.Q., Xiao, T.F., 2005. Mercury emission to atmosphere from lanmuchang hg-tl mining area, southwestern Guizhou, China. Atmos. Environ. 39, 7459–7473.
Wang, S.F., Feng, X.B., Qiu, G.L., Fu, X.W., Wei, Z.Q., 2007. Characteristics of mercury exchange flux between soil and air in the heavily air-polluted area, eastern Guizhou, China. Atmos. Environ. 41, 5584–5594.
Wang, X., Yuan, W., Lu, Z., Lin, C.J., Yin, R., Li, F., et al., 2019. Effects of precipitation on mercury accumulation on subtropical montane forest floor: implications on climate forcing. Journal of Geophysical Research: Biogeosciences 124, 959–972.
Witt, E.L., Kolka, R.K., Nater, E.A., Wickman, T.R., 2009. Influence of the forest canopy on total and methyl mercury deposition in the boreal forest. Water Air Soil Poll 199, 3–11.
Wright, L.P., Zhang, L.M., Marsik, F.J., 2016. Overview of mercury dry deposition, litterfall, and throughfall studies. Atmos. Chem. Phys. 16, 13399–13416.
Yan, J., Wang, C., Wang, Z., Yang, S., Li, P., 2019. Mercury concentration and speciation in mine wastes in Tongren mercury mining area, Southwest China and environmental effects. Appl. Geochem. 106, 112–119.
Yuan, W., Wang, X., Lin, C.J., Jonas, S., Lu, Z.Y., Feng, X.B., 2019. Process factors driving dynamic exchange of elemental mercury vapor over soil in broadleaf forest ecosystems. Atmos. Environ. 219, 352–372.
Zhang, L., Wang, S.X., Wang, L., Wu, Y., Duan, L., Wu, Q.R., et al., 2015. Updated emission inventories for speciated atmospheric mercury from anthropogenic sources in China. Environ Sci Technol 49, 3185–3194.
Zhang, L., Wu, Z., Cheng, I., Wright, L.P., Olson, M.L., Gay, D.A., et al., 2016. The estimated six-year mercury dry deposition across north america. Environ Sci Technol 50, 12864–12873.
Zhao, M., Zeng, C., Liu, Z., Wang, S., 2010. Effect of different land use/land cover on karst hydrogeochemistry: a paired catchment study of chenqi and dengzhanhe, puding, Guizhou, sw China. J. Hydrol. 388, 121–130.
Zhou, J., Wang, Z.W., Zhang, X.S., Gao, Y., 2017. Mercury concentrations and pools in four adjacent coniferous and deciduous upland forests in Beijing, China. J Geophys Res-Biogeo 122, 1260–1274.
Zhou, J., Du, B.Y., Shang, L.H., Wang, Z.W., Cui, H.B., Fan, X.J., et al., 2019. Mercury fluxes, budgets, and pools in forest ecosystems of china: a review. Crit. Rev. Environ. Sci. Technol. 50, 1411–1450.
Zhu, W., Sommar, J., Lin, C.J., Feng, X., 2015. Mercury vapor air-surface exchange measured by collocated micrometeorological and enclosure methods - part ii: Bias and uncertainty analysis. Atmos. Chem. Phys. 15, 5359–5376.
Zhu, W., Lin, C.-J., Wang, X., Sommar, J., Fu, X., Feng, X., 2016. Global observations and modeling of atmosphere–surface exchange of elemental mercury: a critical review. Atmos. Chem. Phys. 16, 4451–4480.